Spatial photoluminescence and lifetime mappings of quasi-2D perovskites coupled with a dielectric metasurface

Hai Xuan Son Bui [1,2], Tuyet Thi Doan[1], Nhan Ha Tri Luong[1], Dang Khue Luu[1], Ha Thi Thu Do[3], Linh Ha Chu[1], Duong Pham[4], Oanh Thi Kim Vu[2], Son Tung Bui[2], Thuat Tran Nguyen[5], Xuan Khuyen Bui[6], Dinh Lam Vu[2], Hai Son Nguyen[7,8], Tung Son Ha[3], Quynh Le-Van[1,*]

[1]*Center for Environmental Intelligence, College of Engineering and Computer Science, VinUniversity, Gia Lam district, Hanoi 14000, Vietnam*
[2]*Graduate University of Science and Technology, 18 Hoang Quoc Viet Street, Hanoi, Vietnam*
[3]*Institute of Materials Research and Engineering, Agency for Science Technology and Research (A*STAR), 2 Fusionopolis Way, Singapore 138634*
[4]*Institute of Physics, Vietnam Academy of Science and Technology, 10 Dao Tan Street, Hanoi, Vietnam*
[5]*Nano and Energy Center, VNU University of Science, 334 Nguyen Trai, Hanoi, Vietnam*
[6]*Institute of Materials Science, Vietnam Academy of Science and Technology, 18 Hoang Quoc Viet street, Hanoi, Vietnam*
[7]*Univ Lyon, Ecole Centrale de Lyon, CNRS, INSA Lyon, Université Claude Bernard Lyon 1, CPE Lyon, CNRS, INL, UMR5270, 69130 Ecully, France*
[8]*IInstitut Universitaire de France (IUF), Paris, France*
[*]*quynh.lv@vinuni.edu.vn*

Abstract: Light-matter interaction between quantum emitters and optical cavities plays a vital role in fundamental quantum photonics and the development of optoelectronics. Resonant metasurfaces are proven to be an efficient platform for tailoring the spontaneous emission (SE) of the emitters. In this work, we study the interplay between quasi-2D perovskites and dielectric TiO_2 metasurfaces.The metasurface, functioning as an open cavity, enhances electric fields near its plane, thereby influencing the emissions of the perovskite. This is verified through angle-resolved photoluminescence (PL) studies. We also conducted reflectivity measurements and numerical simulations to validate the coupling between the quasi-2D perovskites and photonic modes. Notably, our work introduces a spatial mapping approach to study Purcell enhancement. Using Fluorescence Lifetime Imaging Microscopy (FLIM), we directly link the PL and lifetimes of the quasi-2D perovskites in spatial distribution when positioned on the metasurface. This correlation provides unprecedented insights into emitter distribution and emitter-resonator interactions. The methodology opens a new approach for studies in quantum optics, optoelectronics, and medical imaging by enabling spatial mapping of both PL intensity and lifetime, differentiating between uncoupled quantum emitters and those coupled with different types of resonators.

Nanoscale quantum emitters are crucial components in quantum optics, medical science, and optoelectronic research. The control of these emitters is so essential that it has attracted wide-ranging research across scientific domains, from colloidal chemistry to resonator design. Purcell's seminar work demonstrated that the emission rate of emitters is not only an intrinsic feature but also depends on the surrounding electromagnetic fields [1]. Since then, various types of resonators, including photonic crystals [2–5], microcavities [6], hyperbolic metamaterials [7,8], plasmonics [9–15], and dielectric metasurfaces [16–28], have been proposed to tailor the optical properties of quantum emitters through light-matter interaction. In nanophotonics, incorporating quantum emitters in resonant metasurfaces made from arrangements of subwavelength-scale plasmonic or dielectric scatterers has opened new paradigms for novel light sources. Initially, tailoring SE in the resonators was explored in nanoplasmonics [9–11, 15, 29, 30]. The field then

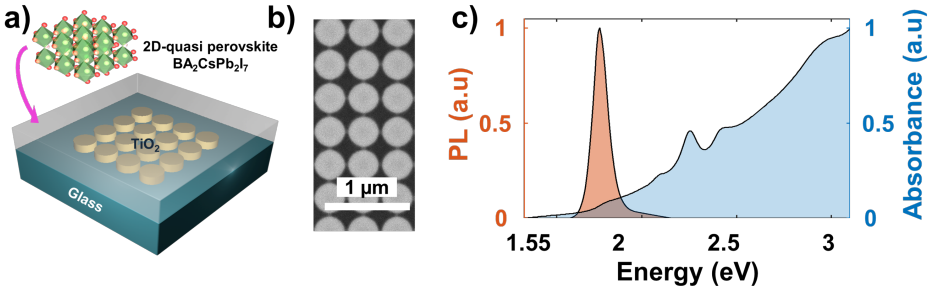

Fig. 1. a) Schematic of the device. A quasi-2D perovskite-doped polymer covered a TiO_2 metasurface on glass substrate. b) SEM image of TiO_2 metasurface. c) Normalized PL and absorbance spectra of the quasi-2D Ruddlesden–Popper perovskites [$BA_2CsPb_2I_7$ with n = 2] embedded in a thin (260 nm thick) polymer film.

shifted toward dielectric metasurfaces with spatially localized Mie resonances, exhibiting low non-radiative losses [17, 18, 27, 31–34].

To elucidate the SE enhancement with metasurfaces, one usually presents the PL of emitters coupled with resonators normalized by the PL of bare emitters [19, 20, 23, 26, 35, 36] and/or the corresponding lifetime of the emitters [21, 26]. However, time-resolved measurements to obtain emitters' lifetimes are typically performed at a single focused point. Thus, the values are considered to represent an ensemble of the emitters. This approach prevents an inaccurate depiction of how the PL and lifetime are spatially defined across the entire metasurface.

Here, we present a direct spatial correlation between the PL enhancement and reduced lifetime of a red emission quasi-2D Ruddlesden–Popper perovskites when positioned on a dielectric TiO_2 metasurface. Our angle-resolved PL and reflectivity measurements reveal that the metasurface can control the polarization, directivity, and intensity of the perovskites via the Purcell effect. A numerical simulation is performed to elucidate these observations with perfect agreement. Most importantly, we present a novel method for spatial mapping of the Purcell enhancement with FLIM. We show a good agreement between the PL intensity and the lifetime of the quasi-2D perovskites in their spatial arrangement on the metasurface. This result offers a unique and detailed understanding of the distribution of emitters and their interactions with delocalized photonic resonances.

The system in this work, depicted in Fig. 1a, consists of a 50 µm x 50 µm TiO_2 metasurface on a glass substrate and a homogeneous ensemble of n-butylammonium cesium lead iodide ($BA_2CsPb_2I_7$) quasi-2D Ruddlesden–Popper perovskites (quasi-2D perovskites) embedded in a mixture of polymers. The TiO_2 metasurface is designed to act as an open cavity that provides the leaked electric fields. To do that, we define the TiO_2 metasurface with a high filling factor (unit cell a = 450 nm, the TiO_2 cylinder with height h = 100 nm and radius r = 210 nm, giving a filling factor ff = 68.42%); thus, less space is available for filling the emitters in the plane of the TiO_2 array. The metasurface, whose scanning electron image is displayed in Fig. 1b, is fabricated by two main procedures: (i) atomic layer deposition is used to make a thin layer of low-lossy TiO_2 material, and (ii) electron beam lithography is deployed to define the structures in the resist layer and then transfer them to TiO_2 layer by dry etching. The fabrication processes presented in Section 1 of the supplementary information (SI) are similar to those in Ref [37]. The ensembles of the quasi-2D perovskite emitters are synthesized following the procedures reported in Ref [38] and details of the synthesis can be found in Section 2 of the SI. The quasi-2D layers of the perovskites and the large filling factor of the metasurface are expected to limit the accommodation of the emitters in the plane of the metasurface. The quasi-2D perovskites are

mixed in a sealed vial with a co-polymer mixture (PMMA 5% wt and PVDF 3% wt) with a volume ratio of 1:9, respectively. A thin layer (≈ 260 nm) of the quasi-2D was obtained by spin coating the solution, followed by soft baking at 140°C under ambient conditions. Figure 1c shows the PL property of the perovskite with a peak at E ≈ 1.75 eV (λ = 710 nm) and a linewidth ≈ 185 meV. The absorption spectrum exhibits a peak at round 550 nm which is consistent with report in Ref [39]. It is noted that using a polymer matrix to retain their emission properties is highly recommended due to high humidity exposure (>70%).

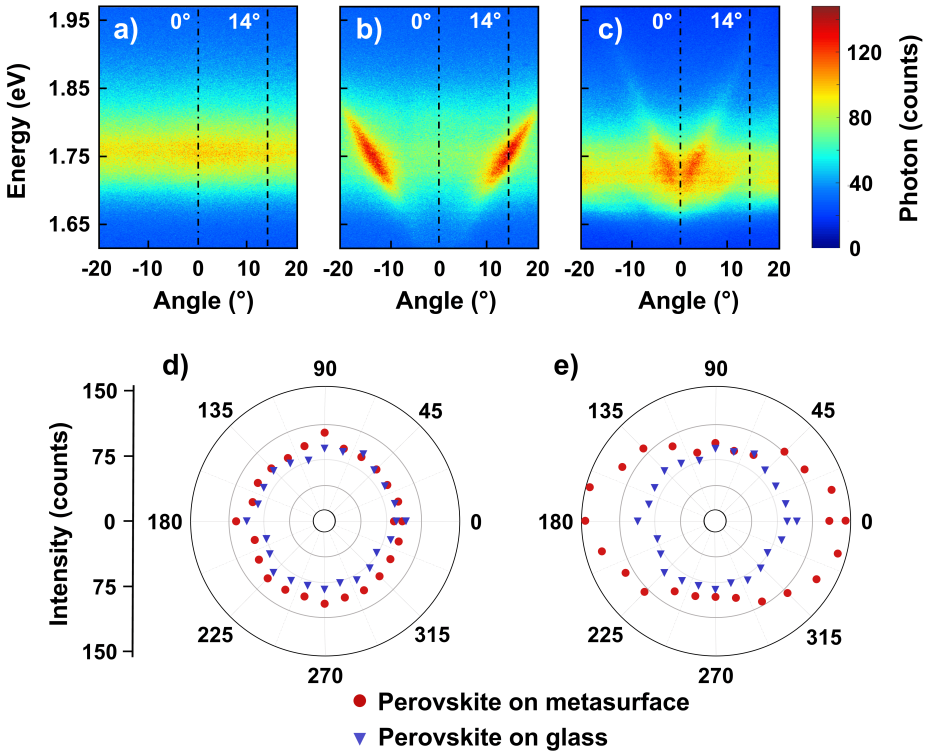

Fig. 2. Angle-resolved PL spectra. a) Angle-resolved PL of uncoupled perovskites in a thin film. The angle-resolved PL of the quasi-2D perovskites coupling with the TiO_2 metasurface is analyzed in b) S-polarization (S-pol) and c) P-polarization (P-pol). The dash dot and dash lines at 0° and 14°, respectively, are the truncated spectra that will be analyzed with polarization set. Analysis of the spectra for the bare perovskites and perovskite-TiO_2 metasurface at d) 0° and e) 14°.

We first studied the angle-resolved PL of the bare quasi-2D perovskite film and the perovskites coupled with the metasurface. We optically excite the system by a continuous laser (λ = 405 nm). The emitted signal from the objective's back-focal plane is directed onto a narrow slit in the monochromator (Princeton Instrument HRS-300) and recorded by spectral camera (Kuro model). The measurement setup is discussed in detailed in Fig. S2 of SI. Figure 2a shows an angle-resolved PL of uncoupled perovskites with the peak centered at 1.75 eV. This PL is independent of the polarization, which reflects the typical characteristics of the SE of the emitters. However, once we switch to the perovskites on top of the metasurface, we observe the polarization dependence of the emission; see Figs. 2b and 2c. Particularly, the angle-resolved PL shows completely different patterns once we observe it in S-polarization (Fig. 2b) and P-polarization (Fig. 2c) modes by tuning the polarizer. Figure 2b displays the PL peak at the same energy level

(E = 1.75 eV) as that of uncoupled perovskites, yet the intensity of PL is augmented in angles from 10°- 20° and the two enhanced lobes are symmetric via the normal incidence. Figure 2c, in contrast, shows a rather different pattern in which the emission peak is red-shifted (centered at 1.72 eV), and the enhanced intensity is observed at smaller angles (1° - 5°). Notably, the PL enhancement, defined as the ratio between PL signal on and outside metasurface, observed with TE-like mode in S-pol (52.98%) is higher than that with TM-like mode in P-pol (2.56%), see Fig. S4. It refers to a better outcoupling between perovskite's emission and the TE-like photonic mode of the metasurface. To further analyze the polarization dependence PL of the coupled perovskite-metasurface, we performed a series of angle-resolved PL maps at normal incidence 0° (vertical dash-dot line) and the center angle of the PL enhancement in P-pol, 14° (vertical dash line). The intensities of the PL spectra at the truncated angles are shown in Figs. 2d and 2e, respectively. The enhancement factor at normal incidence, or polarization = 0° (Fig. 2d) is relatively constant, whereas it changes significantly (2.56 % at 90° to 52.98 % at 0° or 180°) (Fig. 2e). The analysis of PL measurements showed that the dielectric TiO_2 metasurface can modify the emission of the quasi-2D perovskites in terms of intensity, directivity, and polarization through coupling with the photonic modes sustained in the metasurface.

To quantitatively elucidate the PL properties, we perform angle-resolved reflectivity measurement and numerical simulation of the system. The reflectivity setup is the same as that of PL, except the UV laser is replaced by a broadband lamp (Thorlabs SLS202C). The reflectivities of the metasurface covered by a layer of perovskites with S-pol and P-pol are presented in Figs. 3a and 3b, respectively. The angle-resolved reflectivity greatly agrees with the angle-resolved PL presented in Figs. 2b and 2c. Figure 3a shows the highest intensity values form a diagonal line, TE-like mode, that is symmetric via the normal incidence. A red horizontal dash line indicates the exciton emission energy, and it crosses the TE-like mode at 14°. The vertical lines shown in Fig. 2 are replicated in Fig. 3. The crossing point between the quasi-2D perovskite's emission and reflection lines implies that the photonic mode of the metasurface enhanced the emission and light outcoupling to free space. In the P-pol configuration shown in Fig. 3b, we observe a relatively parabolic mode (TE-like mode) with an energy value of E = 1.63 eV at ± 20° which gradually decreases to E = 1.58 eV at normal incidence. In addition, two dimmer photonic modes (TM-like modes) cross at 0° and E = 1.7 eV, and the branches cross the PL of the perovskites at exactly the energy level and angles observed in Fig. 2c. Therefore, we can prove that the PL intensity and directional modification are attributed to the coupling of the perovskite's SE with photonic modes. Next, we perform the numerical simulation by finite element method (Comsol Multiphysics) of the metasurface covered by a perovskite-contained matrix. A square unit cell with floquet boundary conditions is used in the model; the permittivity of TiO_2 (n = 2.54), and the refractive indexes of the superstrate and substrate are 1.60 and 1.46, respectively. Details of the model are available in Fig. S3 of the SI. Figures 3c and 3d display the simulated reflectivities of the system in S-pol and P-pol, respectively. Our numerical results show great agreement with the measured reflectivity. We sketched the inner structures of the unit cell in Fig. 3e. Figure 3f illustrates the electric field at point A, corresponding to an optical mode that confines energy within the structure. Some of the electric field extends into the perovskite layer, enhancing the emission rate of emitters. Figure 3g shows the electric field of two points B and C laying at the same symmetric point, thus sharing the same nature. An example of the electric field of a point that has no optical mode (point D) is illustrated in Fig. 3h.

Finally, we investigated the spatial distribution of PL and the lifetime of the quasi-2D perovskites on and outside of the metasurface. To perform this, we have deployed a FLIM system (ISS VistaVision, USA). The system is sketched in Fig. S4. The measurement setup consists of a laser source at 405 nm, a Galvo scanning mirror used to probe the sample in x- and y- directions, and an inverted Nikon microscopy (20X objective, NA = 0.75) used to inject and collect the signal and an avalanche photodetector. Figure 4a displays the PL distribution in lateral space across

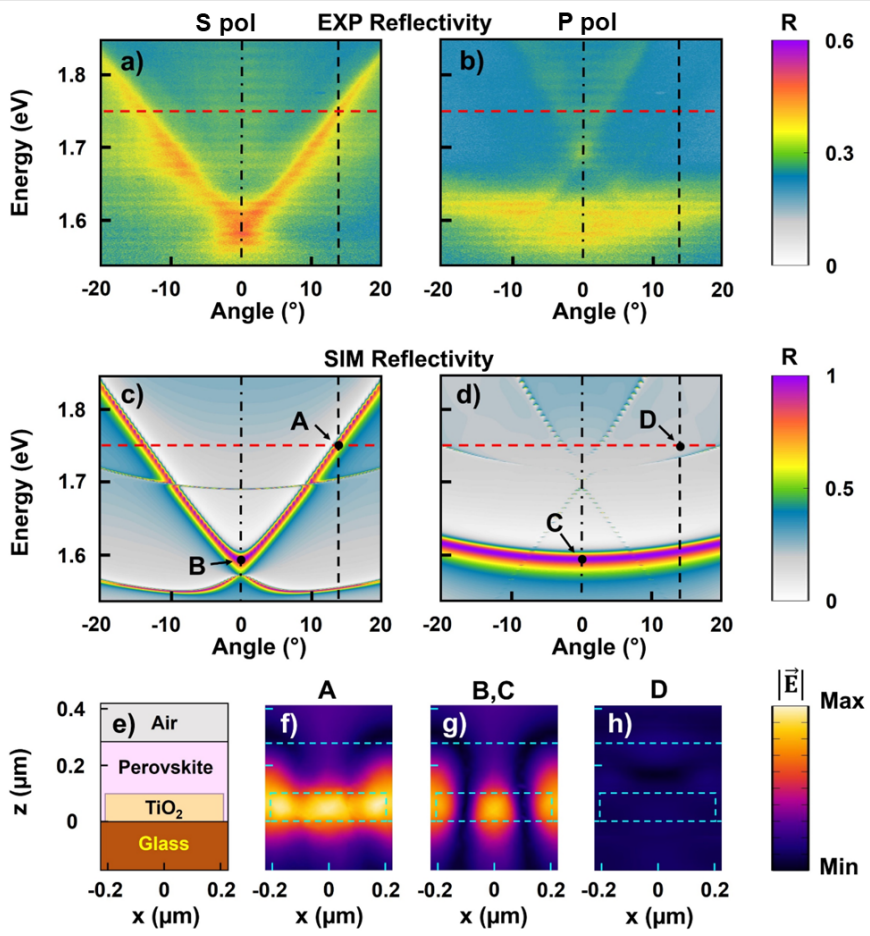

Fig. 3. Angle resolved reflectivity and electric field distribution. The experimental angle-resolved reflectivity in a) S-pol and b) P-pol. The corresponding numerical simulations are in c) and d), respectively. The vertical dash-dot and dash lines correspond to angles 0° and 14°, while the horizontal red dash line (E = 1.75 eV) indicates the spectral peak of the $BA_2CsPb_2I_7$ quasi-2D perovskites. e) shows the side view of the unit cell. Electric fields of four special points A, B, C, and D are displayed in Figs. f–h.

the structures. The size of each pixel is 0.2 μm × 0.2 μm. One can notice a profound contrast between the PL intensity of the perovskites on the metasurface and the bare glass. The enhanced PL on the structure confirms the impact of the enhanced local electric field from the photonic mode on enhancing their fluorescence. In addition, the PL of the bare perovskite layer does not show homogeneity in terms of intensity. This implies that they are not distributed homogeneously, as typically assumed. To study the dynamics of the excitons affected by the resonators, one often measures the lifetime of the electrons in the excited states as an accompanying trait of the Purcell effect. Previous experimental studies have primarily focused on single lifetime measurements to represent the lifetimes of emitter ensembles across the entire metasurface. Unlike a single spot lifetime measurement, our study reveals the lifetime of pixels in two-dimensional space, covering emitters on glass and the structure. We use single exponential fitting for the lifetime, and details of the fitting model for computing the pixel-wide lifetime can be found in Section 5 of the SI. Figure 4b shows the fitted lifetime of the quasi-2D perovskites on and outside of

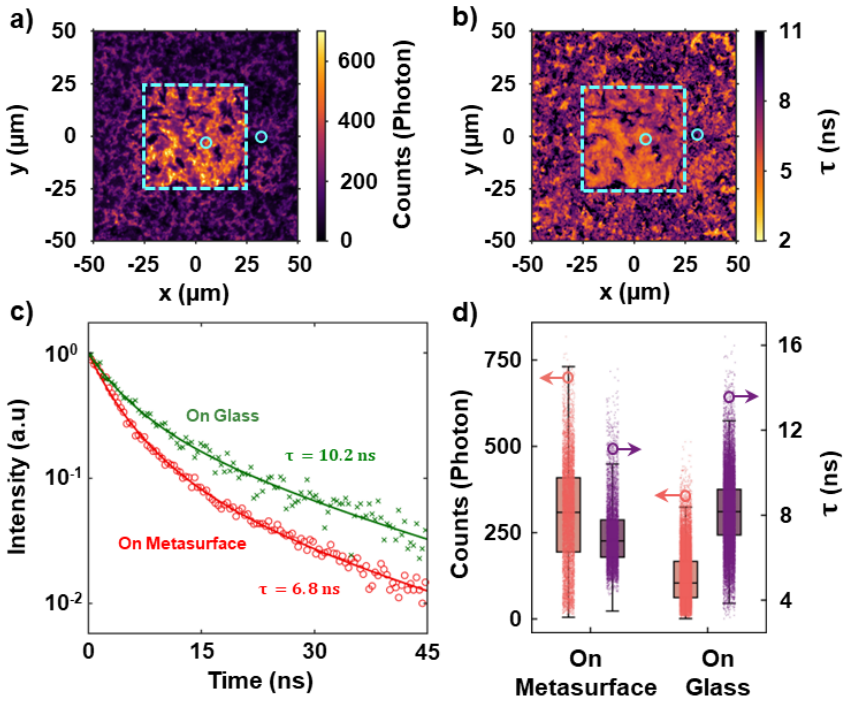

Fig. 4. a) Mapping PL intensity of quasi-2D perovskites on and outside of TiO_2 metasurfaces. b) The lifetime mapping of the corresponded PL intensity mapping in a). c) The PL fittings of two random points on top and outside of the metasurface structure, as indicated by open circles in a). d) The distributions of pixel values for PL intensity and lifetime mappings of the quasi-2D perovskites on and outside of the metasurface.

the structure. The lifetime contrast greatly reflects differences in PL intensity of the perovskites. Overall, the lifetime of the perovskites on the structure is shorter compared to those outside the structure. Figure 4c shows an example of how the lifetime of the perovskites is extracted from the fitted PL intensity at two open circles in Fig. 4a. The lifetime of the perovskites on the metasurface (τ = 6.9 ns) is shorter compared to that on glass (τ = 10.4 ns) which is consistent with the literature [40].

We computed the pixel statistics of the PL intensity and lifetime for the entire frame, as shown in Fig. 4d. The PL intensity of the quasi-2D perovskites on the metasurface was significantly higher than that on glass, with a mean of 310 photons on the metasurface compared to 105 photons on glass. This substantial difference in the mean value of the PL intensity was consistent with the wider interquartile range (IQR) on the metasurface, indicating a broader distribution of PL intensity values. Conversely, a shorter mean lifetime on the metasurface (τ = 6.8 ns) compared to that on glass (τ = 8.2 ns). Such discrepancy between the photon enhancement and lifetime reduction is probably due to the domination of zero-phonon emission rate in the recombination dynamics, i.e., the perovskite emitters have low quantum yield [41]. The metasurface exhibited a narrower IQR for τ, suggesting a more concentrated distribution in the fluorescence lifetimes of the perovskites on the substrate. The measurement indicates that the assemblies of the quasi-2D perovskites doped in polymers demonstrate varying quantum yields, leading to differences in PL enhancement when interacting with the metasurface through the Purcell effect.

In conclusion, our investigation reveals the emission enhancement of $BA_2CsPb_2I_7$ 2D-quasi

perovskites facilitated by the TiO_2 dielectric metasurface. Numerical simulations attribute this Purcell effect to the leakage of electric fields, a factor modifying emissive properties. Furthermore, our measured angle-distributed emission patterns align remarkably well with scattering spectra, reinforcing the efficacy of our metasurface-enhanced approach to tailor the emission rate and direction. We show the direct correlative mapping between PL intensity and the lifetime of perovskites positioned outside and on the metasurface. Though the present study is limited to weak coupling regimes, it could provide valuable insights for studying strong coupling interactions between nanophotonic structures with different types of quantum emitters. Subsequent studies following this work have the potential to make substantial contributions to the realms of optical, biosensing, and medical imaging applications.

Funding: This work was funded by Vingroup Big Data Institute, Vingroup VINIF.2021.DA00169. S.T.H and T.T.H.D acknowledge the funding support from Singapore MTC-Programmatic Grant No: M21J9b0085. S.T.H and AME Young Individual Research Grant No. A2084c0177.
Disclosures: The authors declare no conflicts of interest.
Data availability: Data underlying the results presented in this paper are available upon reasonable request.
Supplemental document: See Supplement 1 for supporting content.

References

1. E. M. Purcell, "Spontaneous emission probabilities at radio frequencies," Phys. Rev. **69**, 681 (1946).
2. S. Noda, M. Fujita, and T. Asano, "Spontaneous-emission control by photonic crystals and nanocavities," Nat. Photonics **1**, 449–458 (2007).
3. P. Lodahl, A. Floris van Driel, I. S. Nikolaev, *et al.*, "Controlling the dynamics of spontaneous emission from quantum dots by photonic crystals," Nature **430**, 654–657 (2004).
4. S. Gupta and E. Waks, "Spontaneous emission enhancement and saturable absorption of colloidal quantum dots coupled to photonic crystal cavity," Opt. Express **21**, 29612–29619 (2013).
5. S.-P. Yu, J. A. Muniz, C.-L. Hung, and H. J. Kimble, "Two-dimensional photonic crystals for engineering atom–light interactions," Proc. National Acad. Sci. **116**, 12743–12751 (2019).
6. T. Jakubczyk, H. Franke, T. Smoleński, *et al.*, "Inhibition and enhancement of the spontaneous emission of quantum dots in micropillar cavities with radial-distributed bragg reflectors," ACS Nano **8**, 9970–9978 (2014).
7. O. Kidwai, S. V. Zhukovsky, and J. E. Sipe, "Dipole radiation near hyperbolic metamaterials: applicability of effective-medium approximation," Opt. Lett. **36**, 2530–2532 (2011).
8. W. Wang, X. Yang, and J. Gao, "Scaling law of purcell factor in hyperbolic metamaterial cavities with dipole excitation," Opt. Lett. **44**, 471–474 (2019).
9. A. Kinkhabwala, Z. Yu, S. Fan, *et al.*, "Large single-molecule fluorescence enhancements produced by a bowtie nanoantenna," Nat. Photonics **3**, 654–657 (2009).
10. C. Belacel, B. Habert, F. Bigourdan, *et al.*, "Controlling spontaneous emission with plasmonic optical patch antennas," Nano Lett. **13**, 1516–1521 (2013).
11. T. B. Hoang, G. M. Akselrod, C. Argyropoulos, *et al.*, "Ultrafast spontaneous emission source using plasmonic nanoantennas," Nat. Commun. **6**, 7788 (2015).
12. Q. Le-Van, X. Le Roux, A. Aassime, and A. Degiron, "Electrically driven optical metamaterials," Nat. Commun. **7**, 12017 (2016).
13. T. B. Hoang, G. M. Akselrod, and M. H. Mikkelsen, "Ultrafast Room-Temperature Single Photon Emission from Quantum Dots Coupled to Plasmonic Nanocavities," Nano Lett. **16**, 270–275 (2016).
14. J. Wang, R. Su, J. Xing, *et al.*, "Room temperature coherently coupled exciton-polaritons in two-dimensional organic-inorganic perovskite," ACS Nano **12**, 8382–8389 (2018).
15. H. Li, F. He, C. Ji, *et al.*, "Purcell-enhanced spontaneous emission from perovskite quantum dots coupled to plasmonic crystal," The J. Phys. Chem. C **123**, 25359–25365 (2019).
16. R. Regmi, J. Berthelot, P. M. Winkler, *et al.*, "All-Dielectric Silicon Nanogap Antennas To Enhance the Fluorescence of Single Molecules," Nano Lett. **16**, 5143–5151 (2016).
17. J. Cambiasso, G. Grinblat, Y. Li, *et al.*, "Bridging the Gap between Dielectric Nanophotonics and the Visible Regime with Effectively Lossless Gallium Phosphide Antennas," Nano Lett. **17**, 1219–1225 (2017).
18. V. Rutckaia, F. Heyroth, A. Novikov, *et al.*, "Quantum Dot Emission Driven by Mie Resonances in Silicon Nanostructures," Nano Lett. **17**, 6886–6892 (2017).
19. N.-V. Hoang, A. Pereira, H. S. Nguyen, *et al.*, "Giant Enhancement of Luminescence Down-Shifting by a Doubly Resonant Rare-Earth-Doped Photonic Metastructure," ACS Photonics **4**, 1705–1712 (2017).

20. A. Vaskin, J. Bohn, K. E. Chong, *et al.*, "Directional and spectral shaping of light emission with mie-resonant silicon nanoantenna arrays," ACS Photonics **5**, 1359–1364 (2018).
21. S. Liu, A. Vaskin, S. Addamane, *et al.*, "Light-emitting metasurfaces: Simultaneous control of spontaneous emission and far-field radiation," Nano Lett. **18**, 6906–6914 (2018).
22. T. Bucher, A. Vaskin, R. Mupparapu, *et al.*, "Tailoring Photoluminescence from MoS2 Monolayers by Mie-Resonant Metasurfaces," ACS Photonics **6**, 1002–1009 (2019).
23. L. Zhu, S. Yuan, C. Zeng, and J. Xia, "Manipulating photoluminescence of carbon g-center in silicon metasurface with optical bound states in the continuum," Adv. Opt. Mater. **8**, 1901830 (2020).
24. N. H. M. Dang, D. Gerace, E. Drouard, *et al.*, "Tailoring dispersion of room-temperature exciton-polaritons with perovskite-based subwavelength metasurfaces," Nano Lett. **20**, 2113–2119 (2020).
25. A. Ndao, L. Hsu, W. Cai, *et al.*, "Differentiating and quantifying exosome secretion from a single cell using quasi-bound states in the continuum," Nanophotonics **9**, 1081–1086 (2020).
26. L. Yuan, J. Jeong, K. W. Chi Kwock, *et al.*, "Manipulation of Exciton Dynamics in Single-Layer WSe2 Using a Toroidal Dielectric Metasurface," Nano Lett. **21**, 9930–9938 (2021).
27. M. Khoury, H. Quard, T. Herzig, *et al.*, "Light emitting si-based mie resonators: Toward a huygens source of quantum emitters," Adv. Opt. Mater. **10**, 2201295 (2022).
28. Y. Xiong, Q. Huang, T. D. Canady, *et al.*, "Photonic crystal enhanced fluorescence emission and blinking suppression for single quantum dot digital resolution biosensing," Nat. Commun. **13**, 4647 (2022).
29. G. Vecchi, V. Giannini, and J. Gómez Rivas, "Shaping the fluorescent emission by lattice resonances in plasmonic crystals of nanoantennas," Phys. Rev. Lett. **102**, 146807 (2009).
30. Q. Le-Van, X. Le Roux, T. V. Teperik, *et al.*, "Temperature dependence of quantum dot fluorescence assisted by plasmonic nanoantennas," Phys. Rev. B **91**, 085412 (2015).
31. B. Gholipour, G. Adamo, D. Cortecchia, *et al.*, "Organometallic perovskite metasurfaces," Adv. Mater. **29**, 1604268 (2017).
32. W. Dai, Y. Wang, R. Li, *et al.*, "Achieving circularly polarized surface emitting perovskite microlasers with all-dielectric metasurfaces," ACS Nano **14**, 17063–17070 (2020). PMID: 33231424.
33. S. Kumar, T. Marcato, F. Krumeich, *et al.*, "Anisotropic nanocrystal superlattices overcoming intrinsic light outcoupling efficiency limit in perovskite quantum dot light-emitting diodes," Nat. Commun. **13**, 2106 (2022).
34. Z. Zhang, C. Xu, C. Liu, *et al.*, "Dual control of enhanced quasi-bound states in the continuum emission from resonant c-si metasurfaces," Nano Lett. **23**, 7584–7592 (2023).
35. S. Yuan, X. Qiu, C. Cui, *et al.*, "Strong Photoluminescence Enhancement in All-Dielectric Fano Metasurface with High Quality Factor," ACS Nano **11**, 10704–10711 (2017).
36. L. Liu, R. Wang, Y. Sun, *et al.*, "Fluorescence enhancement of pbs colloidal quantum dots from silicon metasurfaces sustaining bound states in the continuum," Nanophotonics **12**, 3159–3164 (2023).
37. S. T. Ha, E. Lassalle, X. Liang, *et al.*, "Dual-resonance nanostructures for color downconversion of colloidal quantum emitters," Nano Lett. (2023).
38. H. Lin, J. Mao, M. Qin, *et al.*, "Single-phase alkylammonium cesium lead iodide quasi-2d perovskites for color-tunable and spectrum-stable red leds," Nanoscale **11**, 16907–16918 (2019).
39. J.-F. Liao, H.-S. Rao, B.-X. Chen, *et al.*, "Dimension engineering on cesium lead iodide for efficient and stable perovskite solar cells," J. Mater. Chem. A **5**, 2066–2072 (2017).
40. X. Huang, W. Liu, W. Wang, *et al.*, "Improved phase purity and film quality in quasi-2d perovskite light-emitting diodes by an additive with the trimethacrylate group," RSC Adv. **12**, 3081–3089 (2022).
41. B. Lefaucher, J.-B. Jager, V. Calvo, *et al.*, "Purcell enhancement of silicon w centers in circular bragg grating cavities," ACS Photonics **11**, 24–32 (2024).